Alzheimer's detection through neuro imaging and subsequent fusion for clinical diagnosis

Bhavana Valsala[1], Krishnappa Honnamachanahalli Kariputtaiah[2]
[1]Department of Electronics and Communication Engineering, Amrita School of Engineering, Amrita Vishwa Vidyapeetham,
Bengaluru, India
[2]Department of Computer Science and Engineering, R V College of Engineering, Bengaluru, India

ABSTRACT

In recent years, vast improvement has been observed in the field of medical research. Alzheimer's is the most common cause for dementia. Alzheimer's disease (AD) is a chronic disease with no cure, and it continues to pose a threat to millions of lives worldwide. The main purpose of this study is to detect the presence of AD from magnetic resonance imaging (MRI) scans through neuro imaging and to perform fusion process of both MRI and positron emission tomography (PET) scans of the same patient to obtain a fused image with more detailed information. Detection of AD is done by calculating the gray matter and white matter volumes of the brain and subsequently, a ratio of calculated volume is taken which helps the doctors in deciding whether the patient is affected with or without the disease. Image fusion is carried out after preliminary detection of AD for MRI scan along with PET scan. The main objective is to combine these two images into a single image which contains all the possible information together. The proposed approach yields better results with a peak signal to noise ratio of 60.6 dB, mean square error of 0.0176, entropy of 4.6 and structural similarity index of 0.8.

This is an open access article under the CC BY-SA license.

Corresponding Author:

Bhavana Valsala
Department of Electronics and Communication Engineering, Amrita School of Engineering
Bengaluru, Amrita Vishwa Vidyapeetham, India
Email: bhavanapyarilal@gmail.com

1. INTRODUCTION

Dementia is one of the primary health concerns among the elderly/ageing population in the society. Dementia is a more common term for memory loss and the loss of other cognitive abilities that directly and heavily affect day today life of the suffering person. Alzheimer's disease (AD) is the 7th most common reason for the death of the people all around the world and the most common cause of dementia. In India alone, more than 4 million people suffer from one or the other form of dementia. The first noticeable change of AD is the difficulty in recalling events of a near past, lack of self-care, behavioral changes, and there is no cure for this. The pre-dementia stage symptoms are very similar to that of natural ageing, and hence it is difficult to notice and tell apart these as clear indicators of the disease. According to statistics, about 60-80 percent of all dementia cases evolve into Alzheimer's and detection of AD in its later stages makes it even more tough for the patient and their family to cope with it [1].

There are various imaging modalities that can be used to detect the early biomarkers of Alzheimer's; the typically used techniques are: single photon emission computed tomography (SPECT), positron emission tomography (PET), and magnetic resonance imaging (MRI) [2]. MRI displays tissue information but does not give structural information; this is available in CT scans. PET scans give information regarding the flow of

blood in the area scanned. Research has been done in this area with respect to fusion of images for a final scan that yields more information in comparison with the result of individual imaging modalities. The imaging techniques named are interactive and can be used to highlight specific and different parts of the scanned area [3]. However, individually, they have their own drawbacks.

Several academic reports based on the detection of Alzheimer's using neuroimaging, computer aided diagnostic systems (CADS) and medical image fusion were studied to gain an understanding about the current scenario and the new technologies explored in this research. Anitha *et al.* [4] described the use of image segmentation to detect the disease. Wavelet transform, is used to denoise the image after which a 3-D image is generated; the middle slice of which, is segmented to differentiate white matter (WM) from gray matter (GM) area present and their ratio is calculated leading to a conclusive decision regarding the presence of AD.

Biju *et al.* [5] defined specific ratios obtained by processing MRI scans pertaining to which the state of the brain can be classified into normal, 1st stage Alzheimer's, or 2nd stage Alzheimer's. It follows a method of calculation of WM and GM present in three cross sections of the brain visualized through MR images [6], namely, axial, coronal and sagittal cross sections. An average of the three white and black pixel counts calculated are used to classify the brain scan under different stages of the disease as aforementioned. Taie and Ghonaim [7] described a new model for the early diagnosis of AD based on bat-support vector machine (SVM) classifier. Firstly, features of MRI brain images to build feature vector of brain are obtained. Then the most significant features are extracted using neuroimaging to reduce high dimensional space of MR images and is further classified using machine learning techniques. This bat-SVM model achieved an acceptable accuracy of about 95.36%.

Supriyanti *et al.* [8] has seen a good improvement in analyzing early AD detection with the help of watershed method particularly on coronal slice analysis. The process of identifying images with AD and healthy models are done based on the morphological analysis, by referring to the values of clinical dementia rating (CDR), that has given acceptable results. In the process of fusion, after pre-processing techniques [9]–[13] is applied on an image, it decomposes the images into two components, i.e., approximate coefficients and detailed coefficients. The decomposition happens in both the images and thus, two sets of approximate and detailed coefficients are obtained [14], [15]. These extracted set of approximate coefficients are fused together, and the set of detailed coefficients are fused together and to which fusion rules are applied. To check whether the process holds good or not, the reconstruction process is performed to determine the loss in the mutual information. This involves the use of Haar transform. Image fusion improves the accuracy of detection and the probability of detecting small changes is very high with this process [16], [17].

Multimodal medical image fusion [18] has seen a rise in medical imaging because single modality images lack the ability to provide all the information required in accurately diagnosing a disease. Image fusion techniques proposed includes incorporation of benefits of cross correlation and even degree coefficient fusion along with discrete wavelet transform (DWT) to enhance fused output [19]. The source images are first pre-processed by splitting color channels of PET image, decomposing it into its intensity, hue, and saturation (HIS) transforms and performing DWT [20]–[24] that yields coefficients which are then fused, and inverse transformed back to original hue and saturation coordinates yielding final outputs [25], [26]. This work was evaluated using performance metrics studied in existing literatures namely peak signal to noise ratio (PSNR) and root mean square error (RMSE) [27]. PET image is decomposed into its IHS transform and using this proposed IHS substitution process, fused image is identified to have enhanced anatomical and clinical data. The high frequency coefficient of MRI and PET images is combined with the transformation later using the averaging technique. Inverse DWT is performed to get the resultant fused output [28]–[31].

A modern multi-modal image fusion approach was used in this study [32] to incorporate the benefits of cross correlation and even degree approaches into image fusion techniques. Firstly, two source images are read. PET images are decomposed into its respective color channels and DWT. Even degree method is used to fuse the low and high frequency coefficients. To obtain a fused intensity image, inverse DWT is applied to the fused coefficients. Finally, new intensity image coordinate is interpreted into red, green, blue (RGB) coordinates with its original hue and saturation coordinates to generate a fused image. Diagnosis of Alzheimer's at an early stage provides a better chance of benefiting the individual from treatment. These include heart disease, diabetes, stroke, high blood pressure, high cholesterol, even obesity which aims at proposing a computer aided diagnosis system (CADS) for the detection and diagnosis of AD using neuroimaging followed by fusion of AD detected MRI with PET scans which results in an image that contains the structural information and anatomical information, of both scans respectively, enabling physicians to provide a more informed diagnosis.

The rest of the paper is organized as follows. Section 2 details the proposed approaches of Alzheimer's detection and fusion implementation and explains the steps involved and its architecture. Section 3 explains the results and analysis of the model and compares their performance metrics. Section 4 concludes the work implemented in this paper and describes the future scope.

2. PROPOSED METHOD

The input dataset consists of axial, coronal, and sagittal T1 weighted 256×256 sized MRI brain scans. These datasets are obtained from the Harvard Brain Atlas website. The implementation of this work is conducted using a subset of 6 brain scans, three healthy brain scans and three abnormal brain scans. The implementation of this work is developed and assessed using MATLAB and OpenCV. The abnormal brain scans are those of Alzheimer infected brains. Figure 1 represents the block diagram depicting the method of detection of AD. Method to detect AD consists of image pre-processing as its first step. The main aim is to perform operations on the images at the most basic level to enhance image features and suppress any undesired distortions and noise components without changing the image information content. The operations include image conversion, image resizing, intensity adjustment, filtering and noise removal and histogram equalization.
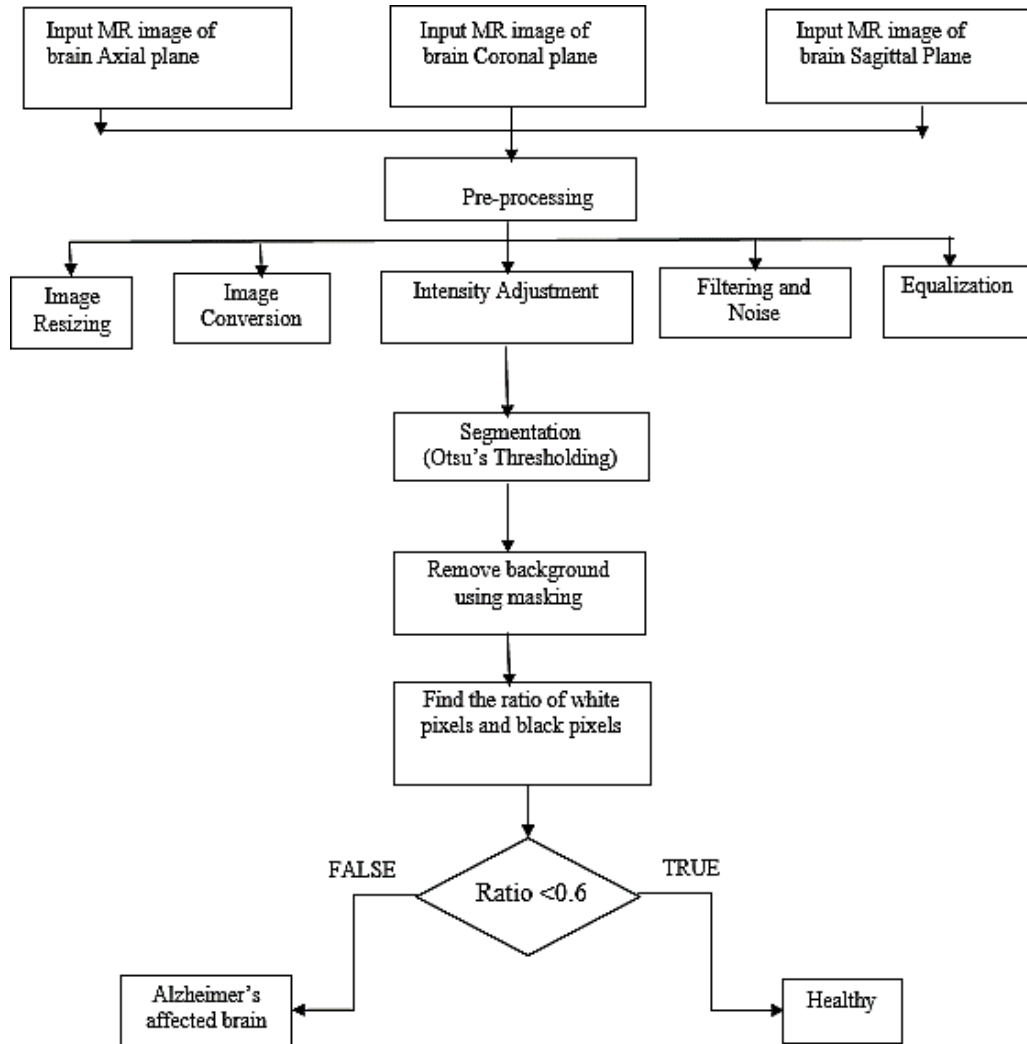

Figure 1. Block diagram depicting method of detection of AD

Filtering, as for one-dimensional signals, can also be used to process images i.e., images can be passed through low-pass filters (LPF) and high-pass filters (HPF). LPF helps to remove noise by making images blurred. High pass filters help to find edges in images. The transfer function for the ideal low pass filter can be given as:

$$H(x,y) = \begin{cases} 1 \ if \ D(x,y) < Do \\ 0 \ if \ D(x,y) > Do \end{cases} \qquad (1)$$

where *Do* is a positive constant, all frequencies within the circle of radius *Do* is passed by the filter, which is termed as the cut-off frequency. *D(x,y)* is the Euclidean distance from any point on the frequency plane to the

origin. A high pass filter is used to sharpen images, i.e., it passes all frequencies above the cut-off value *Do*, having transfer function.

$$H(x,y) = \begin{cases} 0 \ if \ D(x,y) < Do \\ 1 \ if \ D(x,y) > Do \end{cases} \tag{2}$$

Histogram equalization is a technique of image processing that is used to enhance the contrast in images. This is accomplished by evenly distributing the intensity values of the most frequent occurrences. Input pixel intensity, *x* is transformed to a new value *x′* by *T*. *T* is the transform function that is the product of a cumulative histogram and a scale factor:

$$x' = T(x) = \sum_{i=1}^{x} n_i \frac{max.intensity}{N} \tag{3}$$

where number of pixels at intensity *i* is depicted by n_i and the total number of pixels in the image by *N*. This process allows areas of lower local contrast to achieve a higher contrast

Image segmentation is then performed to differentiate WM from GM followed by skull stripping to remove the skull from the scan and avoid calculation of the skull portion as extra white pixels. Otsu's thresholding algorithm is used to implement clustering automatically by reducing gray image to a binary image which proves to be the most efficient for required threshold calculation. The algorithm iteratively searches for a threshold that minimizes the within-class variance of the background (*<threshold*) and foreground (*>threshold*). Class variance is defined as:

$$\sigma^2(t) = \omega bg(t)\sigma^2 bg(t) + \omega fg(t)\sigma^2 fg(t) \tag{4}$$

where $\omega bg(t)$ and $\omega fg(t)$ represents the probability of number of pixels for each class at threshold *t* and σ^2 represents variance of color values.

The skull stripping method behaves as a preliminary step in various medical applications. It boosts precision of diagnosis and gets rid of non-cerebral tissues like skull, scalp, and dura from brain images. Thereby, an algorithm of skull stripping produces a mask that is overlapped onto the original image and the largest connected component is extracted, i.e., the brain. This is followed by masking to remove the unnecessary background portion of skull stripped image. Then the amount of GM and WM are calculated for all three cross-sections and the resultant volume of GM and WM is obtained. The overall brain volume is obtained by adding the volume of all the planes. Experimental findings show that if the ratio is more than 0.6, then the person is normal; if the ratio is less than 0.6, then the person is AD affected.

Image fusion of PET and MRI, at its onset, consists of image denoising using a Gaussian filter and smoothening the entire image. For processing and fusion of gray scaled image with colored image, it is necessary that the images are of the same color scheme. Hence, the RGB scheme PET images are separated into individual red, green and blue channels. Figure 2 represents the process of DWT. Discrete wavelet transform (DWT) is applied to achieve four coefficients, which are LL, LH, HL, and HH coefficients, also known as the approximate and detailed coefficients representing the horizontal and vertical directions of image, respectively.
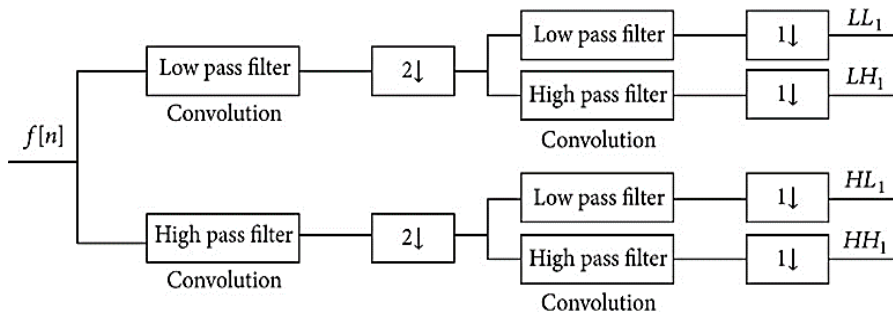

Figure 2. Process of DWT of 2-D image

Figure 3 depicts the block diagram for image fusion. On the individually acquired coefficients for three separate color channels, different fusion rules are applied. Approximation coefficients (LL) of both

MRI and PET scans are fused using one rule and detailed coefficients (LH, HL, HH) are fused using another rule. For e.g., in the case of max-mean rule of fusion, approximation coefficient of PET and MRI are fused using maximum selection rule and the rest of the coefficients are fused using mean selection rule. Nine fusion rules were explored and implemented and finally, it was concluded from the visual outputs yielded that mean-mean fusion rule is more appropriate. Lastly, inverse DWT is applied to fuse all the coefficients back into one image and further fused coefficients of the three different color channels are merged back to form final fused image that contains information of both the MRI and PET images. Final image is evaluated using performance criteria and validated.
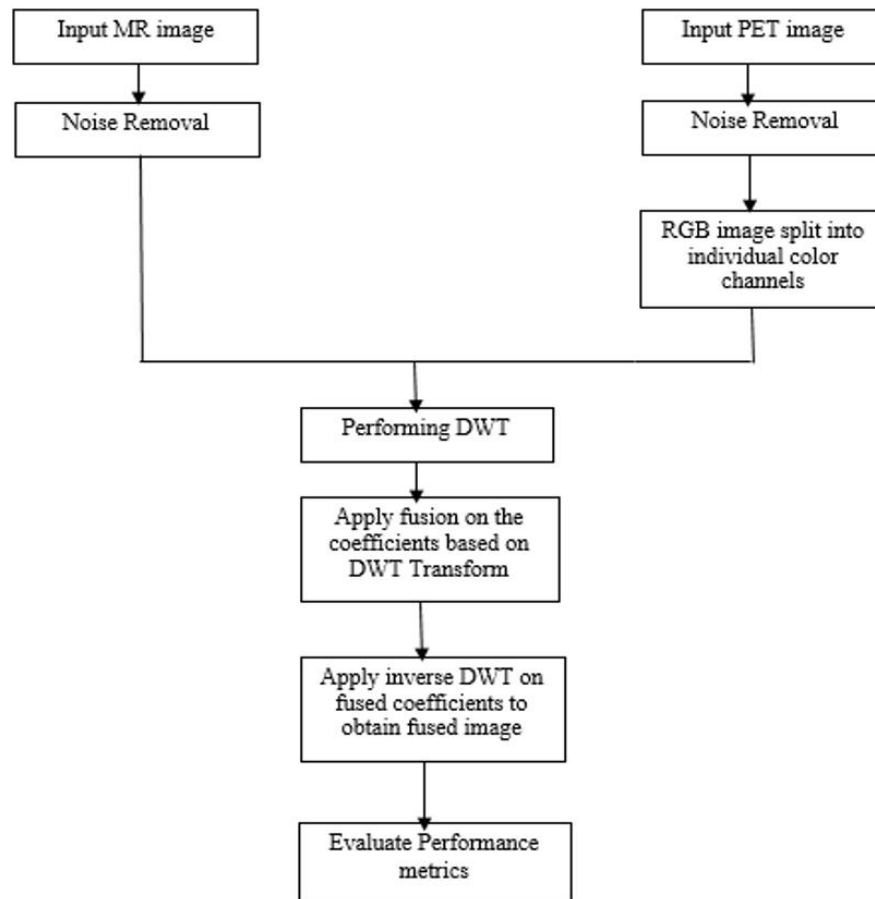

Figure 3. Block diagram depicting method of image fusion

3.   RESULTS AND DISCUSSION

The outputs, and ratios achieved from the MRI scans, yielded from this work have been compared with reference values and is proven to be good.
a. For Axial cross section:
     - Number of white pixels: WM: 391861
     - Number of black pixels: GM: 227314
b. For Coronal cross section:
     - Number of white pixels: WM: 439155
     - Number of black pixels: GM: 179661
c. For Sagittal cross section:
     - Number of white pixels: WM: 437641
     - Number of black pixels: GM: 178552
d. Final ratio: 0.46

Similarly, final ratio for the second dataset used is found to be 0.77. These values are in accordance with the reference values retrieved from related literature survey and from the prior knowledge that the first dataset is from an Alzheimer's patient and the latter of a normal brain is concluded to be accurate.

Alzheimer's detection through neuro imaging and subsequent fusion for clinical diagnosis (Bhavana Valsala)

Further, fusion results have been evaluated with:

a. Entropy: This is an important index to measure the degree of information rich in images. A greater value of entropy indicates that there is higher information content in fused image and is of better quality,

$$entropy = \frac{1}{k}\left(\sum_{i=0}^{255}(p_k(z))log_2(p_k(z))_i\right) \tag{5}$$

where k=R, G, B, and p(z} denoting the probability of ith intensity.

b. Mean square error (MSE): This metric is for measuring image compression quality. MSE represents the cumulative squared error when the fused image is in comparison with the original one. Lower value of MSE indicates lower error.

$$MSE = \frac{1}{MN}\sum_{y=1}^{M}\sum_{X=1}^{N}[(I(x,y) - I'(x,y)]^2 \tag{6}$$

c. PSNR: It is used to figure out the degree of image misrepresentation and is calculated as the ratio of power of the signal to the level of power of the noise. The higher the PSNR value, the better the fusion.

$$PSNR = 10 * log_{10}\frac{(255*255)}{MSE} \tag{7}$$

d. Structural similarity (SSIM) index: It measures quality of fused image with respect to a reference image. It quantifies image degradation cause by processing. Maximum value is +1 and it indicates that the fused and reference image are very similar or same.

$$SSIM(x,y) = [l(x,y)^{\alpha}][c(x,y)^{\beta}][s(x,y)^{\gamma}] \tag{8}$$

The outputs obtained for 3 datasets are depicted in Figures 4 to 6. Performance metrics like entropy, PSNR, MSE, SSIM are calculated for the fusion process using mean-mean fusion rule and has been tabulated as shown in Table 1. The proposed approach yielded good results with performance metric values of PSNR of 60.6 dB, MSE value as low as 0.0176, entropy of 4.6 and SSIM index of 0.8. This methodology helps the medical experts in a larger scale for better clinical diagnosis.
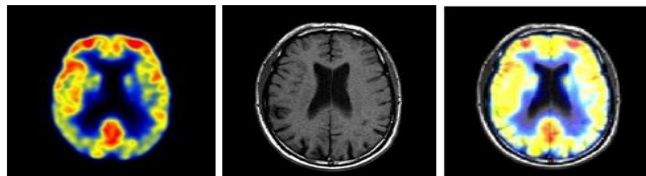

Figure 4. Input PET (left) fused with input MRI (middle) to give final fused output (right) in dataset 1
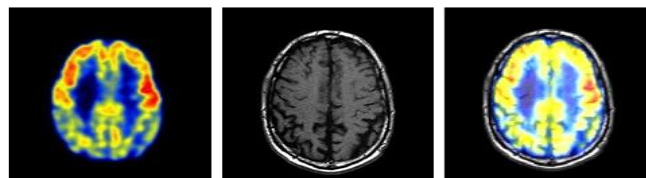

Figure 5. Input PET (left) fused with input MRI (middle) to give final fused output (right) in dataset 2
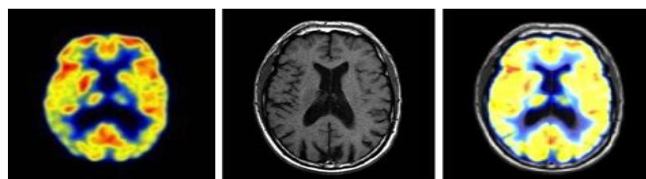

Figure 6. Input PET (left) fused with input MRI (middle) to give final fused output (right) in dataset 3

Table 1. Performance metrics of final outputs

Performance metrics	Dataset 1	Dataset 2	Dataset 3
Entropy of fused image (bits/pixel)	4.6139	3.9779	4.4062
PSNR (dB)	59.6135	60.6098	59.5595
MSE	0.0176	0.0570	0.0725
SSIM	0.7587	0.8083	0.7614

4. CONCLUSION

In this work, we have proposed detection of AD using two different types of brain scans. A comparative study was conducted using T-1 weighted MRI scans of brains, with and without AD. The automated process has very low time complexity. The results overcome the problem of existence of skull portion with respect to other existing methodologies. Detection of AD from scans based on the calculation of area of white and black pixels in the resultant grayscale image and thereby, ratio of the volume of white matter to gray matter output obtained from the algorithm's implementation are found to be in accordance with the reference values collected. Results yielded shows good accuracy with respect to the comparative study of a healthy brain vs not. Image fusion was carried out after preliminary detection of AD for MRI along with PET scans. Pre-processing was carried out for both the scans and 2-level DWT based fusion was implemented. Performance metrics like entropy, PSNR, MSE and SSIM index were used to validate the system which has given promising results. This work can also be extended to use with other imaging modalities such as SPECT, and CT. Two-level DWT has been implemented but higher levels of DWT using other wavelets and fusion of DWT with other methods such as PCA. can be explored to make the fusion outcomes better.

REFERENCES

[1] Z. Maatar, C. Abdelmoula, and M. Masmoudi, "Alzheimer's detection through the association of neuroimaging neuropsychological and clinical data," in *2019 IEEE International Conference on Design & Test of Integrated Micro & Nano-Systems (DTS)*, Apr. 2019, pp. 1–4, doi: 10.1109/DTSS.2019.8914810.

[2] U. R. Acharya *et al.*, "Automated detection of Alzheimer's disease using brain MRI images–A study with various feature extraction techniques," *Journal of Medical Systems*, vol. 43, no. 9, Sep. 2019, doi: 10.1007/s10916-019-1428-9.

[3] V. Bhavana and H. K. Krishnappa, "Multi-modality medical image fusion using discrete wavelet transform," *Procedia Computer Science*, vol. 70, pp. 625–631, 2015, doi: 10.1016/j.procs.2015.10.057.

[4] R. Anitha, S. Jyothi, and P. R. Babu, "Detection of brain abnormality for Alzheimer's disease using image processing techniques," *International Journal of Recent Advances in Engineering & Technology (IJRAET)*, vol. 3, no. 12, pp. 36–40, 2015.

[5] K. S. Biju, S. S. Alfa, K. Lal, A. Antony, and M. K. Akhil, "Alzheimer's detection based on segmentation of MRI image," *Procedia Computer Science*, vol. 115, pp. 474–481, 2017, doi: 10.1016/j.procs.2017.09.088.

[6] M. B. Abdulkareem, "Design and development of multimodal medical image Fusion using discrete wavelet transform," in *2018 Second International Conference on Inventive Communication and Computational Technologies (ICICCT)*, Apr. 2018, pp. 1629–1633, doi: 10.1109/ICICCT.2018.8472997.

[7] S. A. Taie and W. Ghonaim, "A new model for early diagnosis of Alzheimer's disease based on bat-SVM classifier," *Bulletin of Electrical Engineering and Informatics*, vol. 10, no. 2, pp. 759–766, Apr. 2021, doi: 10.11591/eei.v10i2.2714.

[8] R. Supriyanti, A. K. Marchel, Y. Ramadhani, and H. B. Widodo, "Coronal slice segmentation using a watershed method for early identification of people with Alzheimer's," *TELKOMNIKA (Telecommunication Computing Electronics and Control)*, vol. 19, no. 1, pp. 63–72, Feb. 2021, doi: 10.12928/telkomnika.v19i1.15142.

[9] R. Supriyanti, M. Alqaaf, Y. Ramadhani, and H. B. Widodo, "Morphological characteristics of X-ray thorax images of COVID-19 patients using the Bradley thresholding segmentation," *Indonesian Journal of Electrical Engineering and Computer Science (IJEECS)*, vol. 24, no. 2, pp. 1074–1083, Nov. 2021, doi: 10.11591/ijeecs.v24.i2.pp1074-1083.

[10] M. Md Jan, N. Zainal, and S. Jamaludin, "Region of interest-based image retrieval techniques: a review," *IAES International Journal of Artificial Intelligence (IJ-AI)*, vol. 9, no. 3, pp. 520–528, Sep. 2020, doi: 10.11591/ijai.v9.i3.pp520-528.

[11] A. Ashraf, T. Surya Gunawan, B. Subhan Riza, E. V. Haryanto, and Z. Janin, "On the review of image and video-based depression detection using machine learning," *Indonesian Journal of Electrical Engineering and Computer Science (IJEECS)*, vol. 19, no. 3, pp. 1677–1684, Sep. 2020, doi: 10.11591/ijeecs.v19.i3.pp1677-1684.

[12] W. S. Alazawee, Z. H. Naji, and W. T. Ali, "Analyzing and detecting hemorrhagic and ischemic strokebased on bit plane slicing and edge detection algorithms," *Indonesian Journal of Electrical Engineering and Computer Science (IJEECS)*, vol. 25, no. 2, pp. 1003–1010, Feb. 2022, doi: 10.11591/ijeecs.v25.i2.pp1003-1010.

[13] Y. Aufar and I. S. Sitanggang, "Face recognition based on Siamese convolutional neural network using Kivy framework," *Indonesian Journal of Electrical Engineering and Computer Science (IJEECS)*, vol. 26, no. 2, pp. 764–772, May 2022, doi: 10.11591/ijeecs.v26.i2.pp764-772.

[14] V. Bhavana and H. K. Krishnappa, "Fusion of MRI and PET images using DWT and adaptive histogram equalization," in *2016 International Conference on Communication and Signal Processing (ICCSP)*, Apr. 2016, pp. 0795–0798, doi: 10.1109/ICCSP.2016.7754254.

[15] Bhavana V. and Krishnappa H.K., "A survey on multi - modality medical image fusion," in *2016 International Conference on Wireless Communications, Signal Processing and Networking (WiSPNET)*, Mar. 2016, pp. 1326–1329, doi: 10.1109/WiSPNET.2016.7566352.

[16] J. N. Chandra, B. S. Supraja, and V. Bhavana, "A survey on advanced segmentation techniques in image processing applications," in *2017 IEEE International Conference on Computational Intelligence and Computing Research (ICCIC)*, Dec. 2017, pp. 1–5, doi: 10.1109/ICCIC.2017.8524535.

[17] J. N. Chandra, V. Bhavana, and H. . Krishnappa, "Brain tumor detection using threshold and watershed segmentation techniques with isotropic and anisotropic filters," in *2018 International Conference on Communication and Signal Processing (ICCSP)*, Apr. 2018, pp. 0372–0377, doi: 10.1109/ICCSP.2018.8524154.

[18] C. S. Asha, S. Lal, V. P. Gurupur, and P. U. P. Saxena, "Multi-modal medical image fusion with adaptive weighted combination of NSST bands using chaotic grey wolf optimization," *IEEE Access*, vol. 7, pp. 40782–40796, 2019, doi: 10.1109/ACCESS.2019.2908076.

[19] M. M. I. Ch, M. M. Riaz, N. Iltaf, A. Ghafoor, and M. A. Sadiq, "Magnetic resonance and computed tomography image fusion using saliency map and cross bilateral filter," *Signal, Image and Video Processing*, vol. 13, no. 6, pp. 1157–1164, Sep. 2019, doi: 10.1007/s11760-019-01459-8.

[20] R. R. Nair and T. Singh, "Multi-sensor medical image fusion using pyramid-based DWT: a multi-resolution approach," *IET Image Processing*, vol. 13, no. 9, pp. 1447–1459, Jul. 2019, doi: 10.1049/iet-ipr.2018.6556.

[21] V. S. Parvathy and S. Pothiraj, "Multi-modality medical image fusion using hybridization of binary crow search optimization," *Health Care Management Science*, vol. 23, no. 4, pp. 661–669, Dec. 2020, doi: 10.1007/s10729-019-09492-2.

[22] J. Qian, L. Yadong, D. Jindun, F. Xiaofei, and J. Xiuchen, "Image fusion method based on structure-based saliency map and FDST-PCNN framework," *IEEE Access*, vol. 7, pp. 83484–83494, 2019, doi: 10.1109/ACCESS.2019.2924033.

[23] H. R. Shahdoosti and A. Mehrabi, "MRI and PET image fusion using structure tensor and dual ripplet-II transform," *Multimedia Tools and Applications*, vol. 77, no. 17, pp. 22649–22670, Sep. 2018, doi: 10.1007/s11042-017-5067-1.

[24] H. R. Shahdoosti and Z. Tabatabaei, "MRI and PET/SPECT image fusion at feature level using ant colony based segmentation," *Biomedical Signal Processing and Control*, vol. 47, pp. 63–74, Jan. 2019, doi: 10.1016/j.bspc.2018.08.017.

[25] S. Singh and R. S. Anand, "Multimodal neurological image fusion based on adaptive biological inspired neural model in nonsubsampled shearlet domain," *International Journal of Imaging Systems and Technology*, vol. 29, no. 1, pp. 50–64, Mar. 2019, doi: 10.1002/ima.22294.

[26] B. Sun, W. Zhu, C. Luo, K. Hu, Y. Hu, and J. Gao, "Fusion of noisy images based on joint distribution model in dual-tree complex wavelet domain," *International Journal of Imaging Systems and Technology*, vol. 29, no. 1, pp. 29–41, Mar. 2019, doi: 10.1002/ima.22292.

[27] U. S. T. S. and R. P., "Brain tumour detection using discrete wavelet transform based medical image fusion," *Biomedical Research*, vol. 28, no. 2, pp. 684–688, 2017.

[28] L. Wang, X. Dong, X. Cheng, and S. Lin, "An improved coupled dictionary and multi-norm constraint fusion method for CT/MR medical images," *Multimedia Tools and Applications*, vol. 78, no. 1, pp. 929–945, Jan. 2019, doi: 10.1007/s11042-018-5907-7.

[29] K. Xia, H. Yin, and J. Wang, "A novel improved deep convolutional neural network model for medical image fusion," *Cluster Computing*, vol. 22, no. S1, pp. 1515–1527, Jan. 2019, doi: 10.1007/s10586-018-2026-1.

[30] Y. Yang, S. Tong, S. Huang, and P. Lin, "Log-gabor energy based multimodal medical image fusion in NSCT domain," *Computational and Mathematical Methods in Medicine*, vol. 2014, pp. 1–12, 2014, doi: 10.1155/2014/835481.

[31] N. Amini, E. Fatemizadeh, and H. Behnam, "MRI-PET image fusion based on NSCT transform using local energy and local variance fusion rules," *Journal of Medical Engineering & Technology*, vol. 38, no. 4, pp. 211–219, May 2014, doi: 10.3109/03091902.2014.904014.

[32] M. Haribabu, H. Bindu, and K. S. Prasad, "A new approach of medical image fusion using discrete wavelet transform," *ACEEE International Journal of Signal & Image Processing*, vol. 4, no. 2, pp. 21–25, 2013.

BIOGRAPHIES OF AUTHORS

Bhavana Valsala 🆔 🄶 SC ◐ is working as assistant professor (Sr. Gr.) in the Department of Electronics and Communication Engineering, Amrita Vishwa Vidyapeetham, Amrita School of Engineering, Bengaluru. She has a teaching experience of 13 years in the Department of Electronics and Communication Engineering. She is currently pursuing her research in the field of medical image processing. She has published around 20 research articles in reputed journals and conferences. She can be contacted at email: bhavanapyarilal@gmail.com.

Krishnappa Honnamachanahalli Kariputtaiah 🆔 🄶 SC ◐ is working as Associate Professor in the Department of Computer Science and Engineering, R V College of Engineering, Bengaluru. He has a teaching experience of 22 years in the Department of Computer Science and Engineering. He has received his Ph.D. from Visvesvaraya Technological University in the field of graph theory. He has published around 22 research articles in reputed journals and conferences. He can be contacted at krishnappahk@rvce.edu.in.